

See discussions, stats, and author profiles for this publication at: <https://www.researchgate.net/publication/6411075>

NikA Binds Heme: A New Role for an Escherichia coli Periplasmic Nickel-Binding Protein †

ARTICLE *in* BIOCHEMISTRY · JUNE 2007

Impact Factor: 3.02 · DOI: 10.1021/bi700183u · Source: PubMed

CITATIONS

29

READS

31

3 AUTHORS:



[Mark Shepherd](#)

University of Kent

28 PUBLICATIONS 365 CITATIONS

SEE PROFILE



[Matthew Heath](#)

Allergy Therapeutics

12 PUBLICATIONS 66 CITATIONS

SEE PROFILE



[Robert K Poole](#)

The University of Sheffield

332 PUBLICATIONS 9,972 CITATIONS

SEE PROFILE

NikA Binds Heme: A New Role for an *Escherichia coli* Periplasmic Nickel-Binding Protein[†]

Mark Shepherd, Mathew D. Heath, and Robert K. Poole*

Department of Molecular Biology and Biotechnology, The University of Sheffield, Firth Court, Western Bank, Sheffield S10 2TN, U.K.

Received January 29, 2007; Revised Manuscript Received March 9, 2007

ABSTRACT: NikA is a periplasmic binding protein involved in nickel uptake in *Escherichia coli*. NikA was identified as a heme-binding protein in the periplasm of anaerobically grown cells overexpressing CydDC, an ABC transporter that exports reductant to the periplasm. CydDC-overexpressing cells accumulate a heme biosynthesis-derived pigment, P-574. For further biochemical and spectroscopic analysis, unliganded NikA was overexpressed and purified. NikA was found to comigrate with both hemin and protoporphyrin IX during gel filtration. Furthermore, tryptophan fluorescence quenching titrations demonstrated that both hemin and protoporphyrin IX bind to NikA with similar affinity. The binding affinity of NikA for these pigments ($K_d \sim 0.5 \mu\text{M}$) was unaltered in the presence and absence of saturating concentrations of nickel, suggesting that these tetrapyrroles bind to NikA in a manner independent of nickel. To test the hypothesis that NikA is required for periplasmic heme protein assembly, the effects of a *nikA* mutation (*nikA::Tn5*, Km^R insertion) on accumulation of P-574 by CydDC-overexpressing cells was assessed. This mutation significantly lowered P-574 levels, implying that NikA may be involved in P-574 production. Thus, in the reducing environment of the periplasm, NikA may serve as a heme chaperone as well as a periplasmic nickel-binding protein. The docking of heme onto NikA was modeled using the published crystal structure; many of the predicted complexes exhibit a heme-binding cleft remote from the nickel-binding site, which is consistent with the independent binding of nickel and heme. This work has implications for the incorporation of heme into *b*- and *c*-type cytochromes.

Heme, as a prosthetic group in various hemoproteins, is necessary for oxygen transport and storage by hemoglobin and myoglobin. Heme is also essential for electron transport as part of various cytochromes and is also required by mixed function oxidases as a part of cytochrome P-450. Additionally, heme is needed for the decomposition and production of hydrogen peroxide as a cofactor of catalase and peroxidase, respectively (1). Cytochromes are the predominant heme proteins in most prokaryotes. *Escherichia coli* synthesizes heme from 5-aminolevulinic acid via a multistep biosynthetic pathway (2). The incorporation of this metabolically expensive cofactor into *c*-type cytochromes is facilitated by CcmE, a periplasmic chaperone protein that ligates to heme via a single histidine residue (3, 4). However, no such chaperone is known for the synthesis of periplasmic *b*-type cytochromes, such as *E. coli* cytochrome *b*₅₆₂ (5, 6) where heme is bound noncovalently.

The nickel uptake system of *E. coli* encoded by the *nik* operon was originally discovered in mutant strains lacking hydrogenase activity (7, 8). High nickel concentrations could eliminate the defective hydrogenase phenotypes in some of these mutant strains, suggesting a nickel uptake role for the mutated genes. This role was later

confirmed by nickel transport experiments using $^{63}\text{Ni}^{2+}$ (9). Sequencing of the *nik* locus revealed five genes [*nikABCDE* (10)]. NikA is the periplasmic binding protein; the NikB and NikC sequences are similar to integral membrane components of periplasmic permeases, and NikD and NikE possess typical ATP-binding domains, reflecting their likely role in coupling of energy to the transport process. Transcription of the *nik* operon is enhanced under anaerobic conditions via the fumarate and nitrate regulatory protein FNR (8, 10) and is repressed by NikR in the presence of excess nickel (11). The activation of the *nik* operon under anoxic conditions is thought to have evolved to limit the toxic effect of reactive oxygen species that can be generated by nickel in the presence of oxygen (12).

E. coli NikA has been overexpressed and purified, and a K_d value for Ni^{2+} of $<0.1 \mu\text{M}$ was obtained by monitoring the quenching of intrinsic tryptophan fluorescence by the addition of Ni^{2+} (13). However, a more recent study using fluorescently labeled NikA suggested a K_d value of approximately $10 \mu\text{M}$ (14). This weaker binding model was later confirmed by isothermal titration calorimetry (15). The crystal structure of NikA was determined for the unliganded and nickel-bound states (15), which revealed a large nickel-binding cleft where the ligand is largely exposed to the solvent. The authors estimated that periplasmic NikA concentrations are around $120 \mu\text{M}$ so that NikA

[†] This work was supported by Biotechnology and Biological Sciences Research Council (BBSRC) Grant 107647 (to R.K.P.).

* To whom correspondence should be addressed. Telephone: 44-114-222-4447. Fax: 44-114-272-8697. E-mail: r.poole@sheffield.ac.uk.

could exert a significant retentive effect on nickel, despite the relatively high K_d of NikA for the metal ion.

The CydDC transporter of *E. coli* is a heterodimeric ABC transporter that exports cysteine and glutathione to the periplasm (16, 17). This transporter is required for the production of the cytochrome *bd* quinol oxidase (18) and periplasmic *c*- and *b*-type cytochromes (19, 20). The overexpression of CydDC in *E. coli* under anaerobic conditions renders overproducing cells reddish in color and results in the production of a novel pigment with absorption peaks at 448 and 574–579 nm in reduced minus oxidized spectra (21). The formation of this pigment, P-574, is dependent on heme biosynthesis and is the result of enhanced synthesis of the CydDC transporter (21). It was therefore suggested that P-574 may represent a heme–CydDC complex. However, our work reveals that the majority of P-574 is found in the periplasm and is retained by a 50 kDa cutoff filter, implying that this pigment is protein-bound, but not an integral part of membrane protein(s).

This paper describes the binding of heme to NikA and how mutation of NikA can diminish the production of P-574 in anaerobic CydDC-overexpressing cells. Given the expression patterns of NikA and cytochrome *bd*, our data are consistent with a link between the CydDC transporter, NikA, and heme processing during oxidase assembly.

EXPERIMENTAL PROCEDURES

Materials. Protoporphyrin IX was purchased from Frontier Scientific Inc. (formerly Porphyrin Products) (Logan, UT). Hemin, tris(hydroxymethyl)aminomethane carbonate (Tris),¹ and *N*-acetyltryptophanamide (NATA) were purchased from Sigma-Aldrich. All other chemicals were purchased from BDH laboratory supplies (Poole, England) unless otherwise stated.

Porphyrin Preparation. Protoporphyrin IX and hemin were solubilized with a few drops of 30% ammonium hydroxide and then diluted with 50 mM Tris (pH 7.5). Concentrations of protoporphyrin IX were determined in 2.7 N HCl using an ϵ_{554} of $13.5 \text{ mM}^{-1} \text{ cm}^{-1}$ (22). Hemin was quantified using the pyridine hemochrome method as previously described [$\epsilon_{557-541} = 20.7 \text{ mM}^{-1} \text{ cm}^{-1}$ (23)].

Bacterial Strains and Media. The bacterial strains used in this work are described in Table 1. *E. coli* was grown anaerobically in “56” medium (24) supplemented with 0.1% casamino acids. Antibiotics were used where appropriate, and concentrations were 100 and 50 $\mu\text{g/mL}$ for ampicillin and kanamycin, respectively. NikA was overexpressed in the cytoplasm of *E. coli* BL21(DE3)pLysS cells (25) as previously described (15) (strain RKP5509). The pET28b-*nikA* plasmid (15) encodes the mature NikA protein without the 22-amino acid periplasmic-targeting sequence so that overexpressed NikA accumulates in the cytoplasm. Cells were grown in Luria-Bertani (LB) medium with 50 $\mu\text{g/mL}$ kanamycin.

Isolation of Heme-Bound NikA from *cydDC*-Overexpressing Cells. *E. coli* strain RKP2624 cells (Table 1) were grown

Table 1: Strains and Plasmids Used

	relevant genotype	reference or source
<i>E. coli</i> strain		
AN2342	F [−] termed wild type	(50)
BL21(DE3) pLysS	F [−] <i>ompT hsdS_B(_{TS}[−] m_B[−]) gal dcm</i> (DE3) pLysS, Cm ^R	(25)
Δ nikA	MG1655 but <i>nikA::ΩKm^R</i>	Blattner <i>E. coli</i> mutant strain (University of Wisconsin)
RKP2624	As AN2342 but pRKP1602	(21)
RKP5507	As Δ nikA but pRKP1602	this work
RKP5509	BL21(DE3)pLysS but pET28b- <i>nikA</i>	(15)
plasmid		
pET28b- <i>nikA</i>	<i>nikA</i> ⁺ in pET28b, Km ^R	(15)
pRKP1602	<i>cydC</i> ⁺ <i>cydD</i> ⁺ in pBR328, Ap ^R	(21)

in anaerobic flasks at 37 °C for 48 h. The cells were harvested at 4000g for 20 min at 20 °C. In an attempt to induce partial cell lysis while maintaining a reducing environment [P-574 being highly labile (21)], cells were incubated with 50 mM Tris (pH 7.5) and 1 mM DTT and incubated for 30 min with stirring. The soluble fraction was then centrifuged at 39000g for 30 min, and the supernatant was used for chromatographic separation. The lysate was applied to a 15 mL Q-Sepharose anion exchange column (Amersham Biosciences) equilibrated in 50 mM Tris (pH 8.0) and 1 mM DTT, and the column was washed with this buffer at a rate of 2 mL/min until the UV absorbance detector (280 nm) reached the initial baseline. A linear gradient from 0 to 1 M NaCl was passed through the column over 10 column volumes, and absorption spectra of the eluted fractions were recorded. The only absorption spectrum that resembled a heme protein eluted at approximately 100 mM NaCl. This was applied to a Superdex-75 gel filtration column equilibrated in 50 mM Tris (pH 8.0), 1 mM DTT, and 0.1 M NaCl. The separation was performed at a rate of 1 mL/min, and the absorption spectra of eluted protein peaks were recorded. The Superdex-75 column was calibrated with gel filtration molecular weight standards (Sigma).

Overexpression and Purification of NikA from the *E. coli* Cytoplasm. NikA was overexpressed and purified as previously described (15). Purity was confirmed using SDS–PAGE; a single band at 56 kDa was obtained (data not shown).

Absorbance and Fluorescence Spectroscopy. Fluorescence spectra were obtained with a Hitachi F-2500 fluorimeter at room temperature. All spectra were recorded in a 3 mL quartz cuvette in 10 mM Tris (pH 7.3). The excitation wavelength was set to 290 nm, and emission scans were recorded in the range of 310–400 nm. Excitation and emission slits were set to 10 nm. Absorption spectra of purified proteins were recorded using a Cary 50 spectrophotometer in 10 mM Tris (pH 7.3). Reduced (sodium dithionite) minus oxidized (ammonium persulfate) absorption spectra of whole cells in 10 mM Tris (pH 7.3) were recorded at room temperature as described by Poole et al. (18).

Analysis of Apparent Dissociation Constants. Binding titration data were fitted to eq 1, in which a single type of binding site is assumed:

¹ Abbreviations: Ap, ampicillin; Cm, chloramphenicol; DTT, dithiothreitol; Km, kanamycin; NATA, *N*-acetyltryptophanamide; PBP, periplasmic binding protein; PVDF, polyvinylidene fluoride; Tris, tris(hydroxymethyl)aminomethane carbonate.

$$F_{\text{obs}} = F_0 + \frac{F_{\text{max}}}{\frac{[L]_T + [E]_T + K_d - \sqrt{([L]_T + [E]_T + K_d)^2 - 4[L]_T[E]_T}}{2[E]_T}} \quad (1)$$

where F_{obs} is the observed fluorescence, F_0 is the initial fluorescence, F_{max} is the maximum amplitude of fluorescence quenching, $[L]_T$ is the total ligand concentration, $[E]_T$ is the total concentration of protein, and K_d is the apparent dissociation constant.

Determination of N-Terminal Sequence. Proteins were electroblotted onto Problott membranes (Applied Biosystems) before being stained with Coomassie Blue. The N-terminal sequences of the protein bands were determined by sequential Edman degradation (26).

RESULTS

NikA Is Copurified from the *E. coli* Periplasm with Bound Heme. Periplasm was isolated from bacterial cells overexpressing CydDC, and thus accumulating the novel P-574 pigment (RKP2624). Reduced minus oxidized spectra demonstrated that the periplasm contained 5 times more P-574 than the resulting spheroplasts (data not shown). Also, the P-574 signal was retained by a 50 kDa cutoff filter, indicating that the P-574 pigment is protein-bound. In an effort to purify a P-574-bound protein from the *E. coli* periplasm, anion exchange and gel filtration chromatography were used to isolate proteins associated with the P-574 pigment. A P-574-containing supernatant fraction from RKP2624 cells was subjected to anion exchange chromatography. Only one fraction contained an absorption peak around 400–450 nm indicative of heme, and this fraction eluted at approximately 100 mM NaCl. This sample was passed through a Superdex S-75 gel filtration column, and the pigment eluted after 57 mL. This fraction was concentrated and resolved using SDS-PAGE (Figure 1A). The sample was blotted onto a PVDF membrane, and N-terminal sequencing revealed the identity of this 56 kDa band as mature NikA (result, AAPDEI). This corresponds to residues 23–28, as the 22-residue periplasmic targeting sequence is cleaved following translocation. Despite the fact that RKP2624 is not engineered to overexpress NikA, heme could be detected in column fractions only in association with NikA (since cytochrome *c* has an isoelectric point of around pH 10, this protein will be positively charged at pH 8.0 and will not bind to anion exchange resin). The absorption spectrum of this fraction is shown in Figure 1B, where the inset highlights the presence of bound heme. The reduced minus oxidized absorption spectrum of this fraction did not contain P-574, but since this pigment is highly labile (21), it seems plausible that, after two chromatographic steps, this pigment may have converted into a more stable heme compound.

NikA Comigrates with both Hemin and Protoporphyrin IX during Gel Filtration. Purified NikA migrates as a 56 kDa monomer during gel filtration and elutes in the 57 mL fraction from a Superdex-75 gel filtration column (Figure 2A). NikA was overexpressed and purified from the *E. coli* cytoplasm for these experiments. A solution containing 20 μM NikA and 20 μM protoporphyrin IX was applied to the column, and the absorption spectrum for the 57 mL peak revealed the presence of protoporphyrin IX (Figure 2B inset). The Soret absorption peak for bound protoporphyrin was at

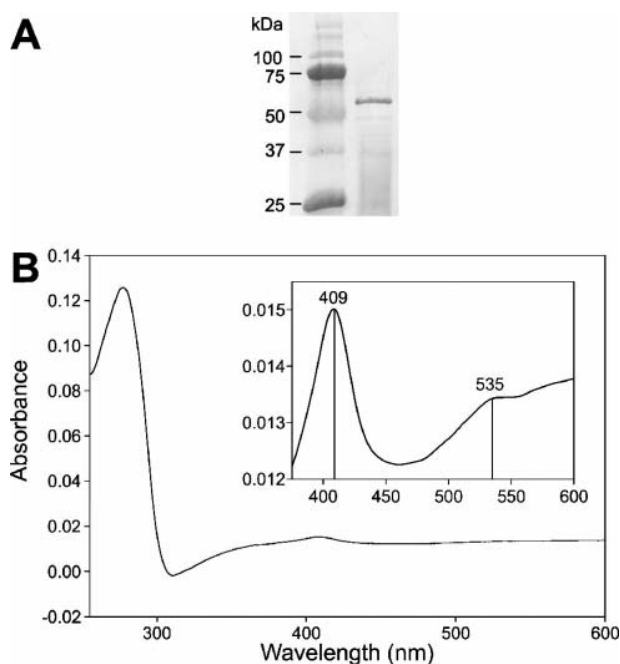


FIGURE 1: Periplasmic NikA copurifies with a bound pigment. (A) SDS-PAGE analysis of NikA purified from the periplasm of cells overexpressing CydDC (RKP2624). (B) Absorption spectra of periplasmic NikA from panel A. The inset highlights the absorption of pigments bound to NikA.

422 nm, and the absorption peaks at 542, 587, and 642 nm correspond to Q-band absorption peaks of protoporphyrin IX. The analogous experiment was performed with 20 μM NikA and 20 μM hemin, which demonstrated that NikA also comigrates with heme (Figure 2C inset). The NikA-heme complex exhibits absorption peaks at 405 and 557 nm. No pigments were detected in 57 mL fractions when only protoporphyrin or hemin was loaded onto the column. These observations strongly suggest that NikA is able to bind both of these tetrapyrrole pigments.

The Binding of NikA to Hemin and Protoporphyrin IX Is Confirmed Using Tryptophan Fluorescence Quenching. NikA was overexpressed and purified from the *E. coli* cytoplasm for these experiments. The binding of NikA to hemin and protoporphyrin was assessed using the perturbation of intrinsic tryptophan fluorescence. NikA (0.1 μM) was excited using 290 nm light, and fluorescence emission was monitored at 330 nm. The addition of either hemin or protoporphyrin resulted in the partial quenching of this fluorescence emission. Samples were incubated for 1 min after the addition of titrant to ensure that no further quenching occurred. Control titrations were performed using *N*-acetyltryptophanamide (NATA) as the fluorophore (27), and the resultant data were used to correct for inner filter effects of the titrant. Figure 3A shows the raw data for typical titrations of NikA and NATA with hemin. Figure 3B shows the decrease in NikA fluorescence after inner filter effects have been subtracted. The black circles represent the titration in the absence of nickel, and the white circles represent the titration in the presence of 100 μM NiCl_2 . Both data sets have been fitted to single rectangular hyperbolae (eq 1), and K_d values of 0.53 ± 0.14 and 0.42 ± 0.14 μM were obtained in the absence and presence of 100 μM nickel, respectively. The analogous titrations were performed with protoporphyrin

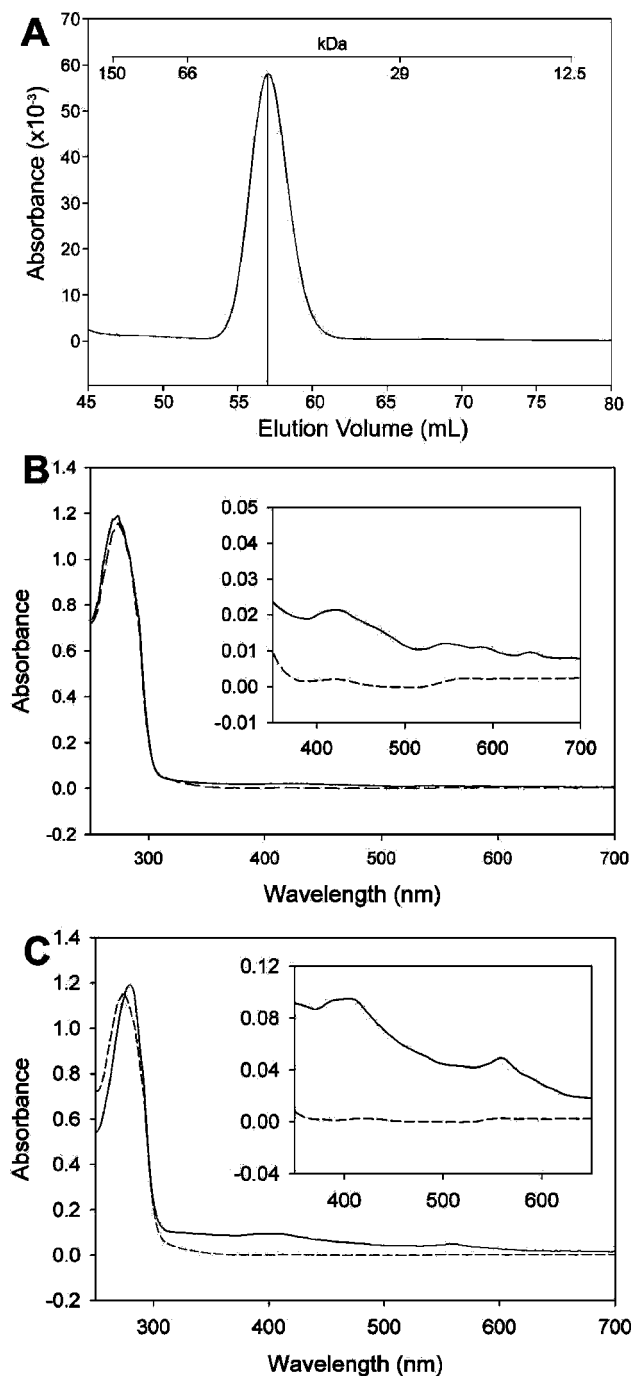


FIGURE 2: NikA coelutes with protoporphyrin IX and hemin during gel filtration. Purified NikA (20 μ M) was preincubated with 20 μ M protoporphyrin IX and 20 μ M hemin and applied to a Sepharose S-75 gel filtration column. (A) A typical chromatogram for 20 μ M NikA. The vertical line in the chromatogram indicates an elution volume of 57 mL. (B) Absorption spectra of 57 mL peaks when NikA (—) and NikA with protoporphyrin IX (---) were applied to the column. (C) Absorption spectra of 57 mL peaks when NikA (---) and NikA with hemin (—) were applied to the column. The insets in panels B and C highlight the absorption of bound pigments.

IX, and K_d values of 0.42 ± 0.06 and 0.54 ± 0.11 μ M were obtained in the absence and presence of 100 μ M nickel, respectively. These data clearly demonstrate that NikA binds to both hemin and protoporphyrin IX, and the presence of a saturating concentration of nickel does not affect these binding affinities. This implies that hemin and protoporphyrin

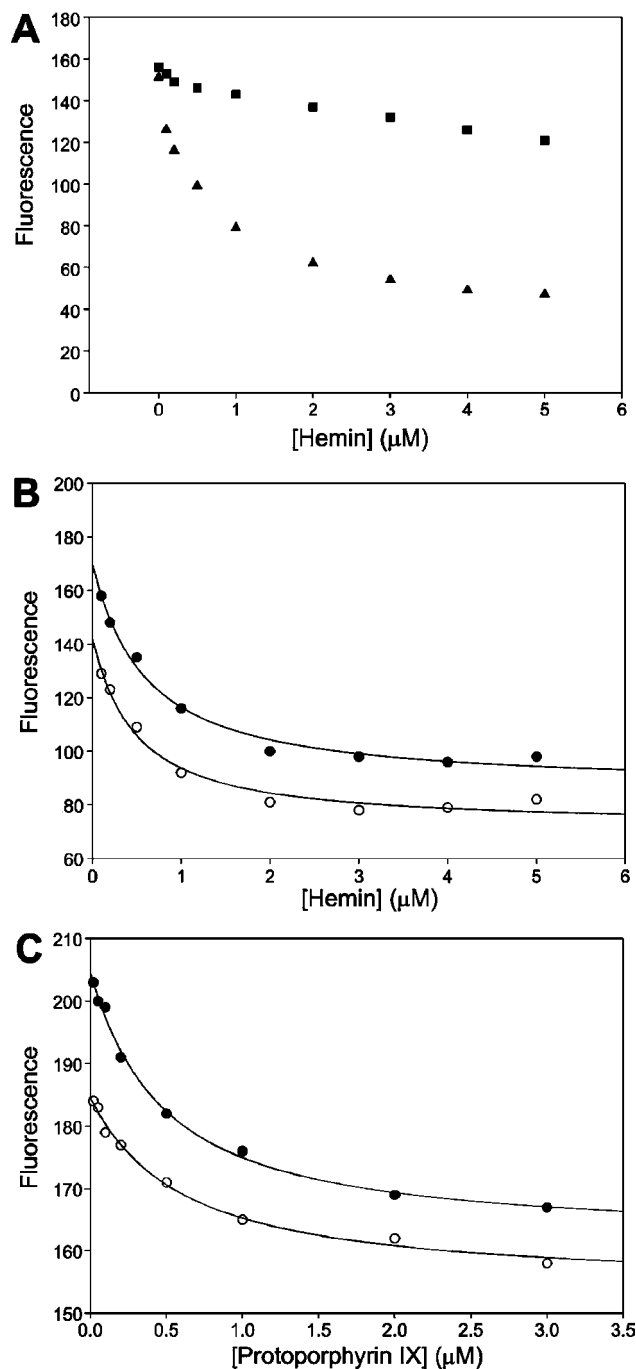


FIGURE 3: Titration of NikA in the presence and absence of 100 μ M Ni^{2+} . (A) Raw fluorescence data for the titration of 0.1 μ M NikA (\blacktriangle) and 0.67 μ M *N*-acetyltryptophanamide (\blacksquare) with hemin, in the presence of 100 μ M Ni^{2+} . (B) NikA was titrated with hemin in the presence (\circ) and absence (\bullet) of 100 μ M Ni^{2+} . $K_d(-\text{Ni}^{2+}) = 0.53 \pm 0.14$ μ M, and $K_d(+100$ μ M $\text{Ni}^{2+}) = 0.42 \pm 0.14$ μ M. (C) NikA was titrated with protoporphyrin IX in the presence (\circ) and absence (\bullet) of 100 μ M Ni^{2+} . $K_d(-\text{Ni}^{2+}) = 0.42 \pm 0.06$ μ M, and $K_d(+100$ μ M $\text{Ni}^{2+}) = 0.54 \pm 0.11$ μ M.

IX bind to NikA at a site remote from the nickel-binding cleft. Nickel binding experiments were performed using tryptophan fluorescence quenching, as a K_d of 0.1 μ M for nickel has previously been reported (13). However, the signal change using this technique was too low to measure K_d values, which is consistent with more recent work (15). It is likely that the lower fluorescence values for the titrations containing nickel in Figure 3 are due to the

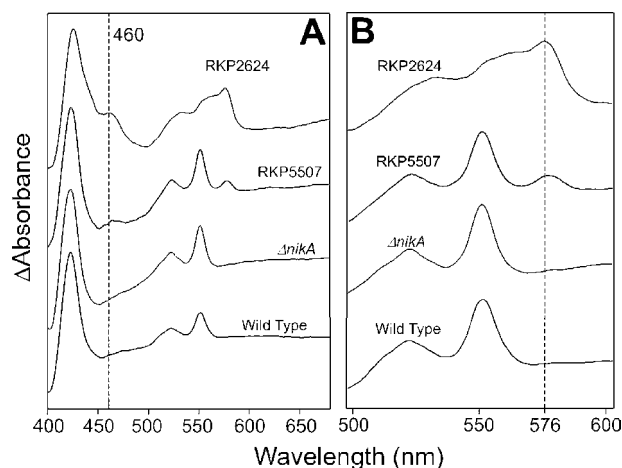


FIGURE 4: Mutation of the *nikA* gene diminishes P-574 levels in a CydDC-overexpressing strain. Whole-cell reduced minus oxidized absorption spectra were recorded for wild-type (AN2342) and Δ *nikA* strains, and the same strains harboring the pRKP1602 plasmid (RKP2624 and RKP5507, respectively). Panel A shows the absorption profiles from 400 to 680 nm and highlights 460 nm with a dashed line. Panel B focuses on the central region of panel A, and 576 nm is highlighted with a dashed line. The spectra were normalized for maximum amplitude change and have been offset for clarity.

absorption of 330 nm fluorescence by the Ni^{2+} ions: NiCl_2 has a Soret absorption peak at 393 nm in aqueous solution, but the broad absorption extends close to 300 nm (data not shown).

NikA Is Required for Maximal Accumulation of P-574. Δ *nikA* cells were transformed with *cydDC*-encoding plasmid pRKP1602 (21) to produce strain RKP5507. Both Δ *nikA* and RKP5507 strains were grown anaerobically, alongside AN2342 (wild type) and RKP2624 (wild type pRKP1602) strains (17). Figure 4 demonstrates that the presence of a *nikA* mutation significantly decreases the presence of P-574 in CydDC-overexpressing cells, implicating NikA in the accumulation of P-574.

Docking of Heme to NikA. Heme was docked onto the structure of *E. coli* NikA (15) using ZDOCK [http://zdock.bu.edu/ (28)]; seven of the 15 predicted complexes were bound to NikA in a cleft remote from the nickel-binding cleft (Figure 5A,B). In four of these complexes, the heme group is situated at the interface between lobes I and II of the protein, and in three of them, the heme is situated on lobe I adjacent to three tryptophan residues (Figure 5C; only one complex is shown for clarity). Figure 5D shows this binding pocket in more detail. Given the proximity of this region to Trp-54 and Trp-63, it is conceivable that a bound heme at this site may elicit the quenching of intrinsic tryptophan fluorescence. This model is consistent with the observation that nickel does not affect the binding of tetrapyrroles to NikA.

DISCUSSION

It has been proposed that the periplasm of wild-type *E. coli* contains approximately 23 000 copies of NikA under anaerobic conditions (13). Assuming the cell to have a volume of $1.6 \mu\text{m}^3$ and 20% of this volume to be periplasmic (13), 23 000 copies is equivalent to $120 \mu\text{M}$ protein. Silhavy et al. (29) used mathematical models to demonstrate that the

rate of diffusion of a ligand out of the periplasm may be decreased by a factor of $1 + [\text{PBP}]/K_d$ when a periplasmic binding protein (PBP) is present in a large excess. Therefore, with a K_d of $0.5 \mu\text{M}$ for heme, $120 \mu\text{M}$ NikA could elicit a 240-fold reduction in the rate of efflux of heme from the periplasm. Since the generation of heme is such an expensive metabolic process (2), it seems reasonable that the cell should possess a mechanism for retaining this valuable cofactor. The covalent attachment of heme groups to periplasmic *c*-type cytochromes in *E. coli* is a complex process involving at least 12 proteins, including the cytochrome *c* maturation (Ccm) system (CcmABCDEFGH) and the DsbA, DsbB, DsbD, and TrxA proteins involved in disulfide bond formation (30–33). The incorporation of noncovalently bound heme into cytochrome b_{562} , the only periplasmic *b*-type cytochrome in *E. coli*, was achieved spontaneously in vitro (34, 35). However, it is not clear how the heme cofactor is delivered to cytochrome b_{562} in vivo. Since heme biosynthesis is maintained during anoxic growth and there is a weakened requirement for cytochrome formation during anaerobic respiration, an anaerobically expressed protein such as NikA might facilitate the retention of surplus periplasmic heme.

The data presented herein clearly demonstrate that NikA binds heme both in vivo and in vitro. The absorption spectra in Figures 1 and 2 are characteristic of a substoichiometric pigment:protein ratio. During the purification of native NikA, there is ample opportunity for the dissociation of the heme–NikA complex, since this complex has been passed down two chromatography columns. Another explanation for this partial binding may be that the concentration of free heme in the periplasm may be below the K_d for binding of NikA to heme ($\sim 0.5 \mu\text{M}$, Figure 3B). The purification of a reconstituted pigment–NikA complex also demonstrated the partial binding of NikA to heme and protoporphyrin (Figure 2). This may be caused by the dissociation of the complex during gel filtration.

The initial aim of this work was to purify a protein-bound P-574 complex. Since NikA was the only protein that was isolated from the *E. coli* periplasm with a heme cofactor, this was a sensible candidate for P-574. Overexpression of CydDC in a *nikA* mutant greatly reduced the P-574 levels in anaerobically grown *E. coli* (Figure 4), which is consistent with the hypothesis that NikA binds heme to generate the P-574 signal. Although purified NikA from the *E. coli* periplasm does bind heme (Figure 1), the reduced minus oxidized spectrum does not contain the P-574 pigment. However, since this pigment is highly labile (21), it may have reverted to a more stable heme compound, resulting in the loss of P-574 signal.

In *E. coli* mutant strains that are deficient in the CydDC transporter, the periplasm becomes “overoxidized” (20). Hence, the overexpression of CydDC may give rise to “over-reduced” conditions in the periplasm. Such conditions may maintain periplasmic thiols in a reduced state, which could inhibit the incorporation of heme into *c*-type cytochromes. This agrees with the observation that glutathione may cleave the thioether bond of cytochrome *c* (36). We propose that the reducing periplasm that results from CydDC overexpression can give rise to an accumulation of *c*-type cytochrome-derived heme, which in turn is retained by NikA,

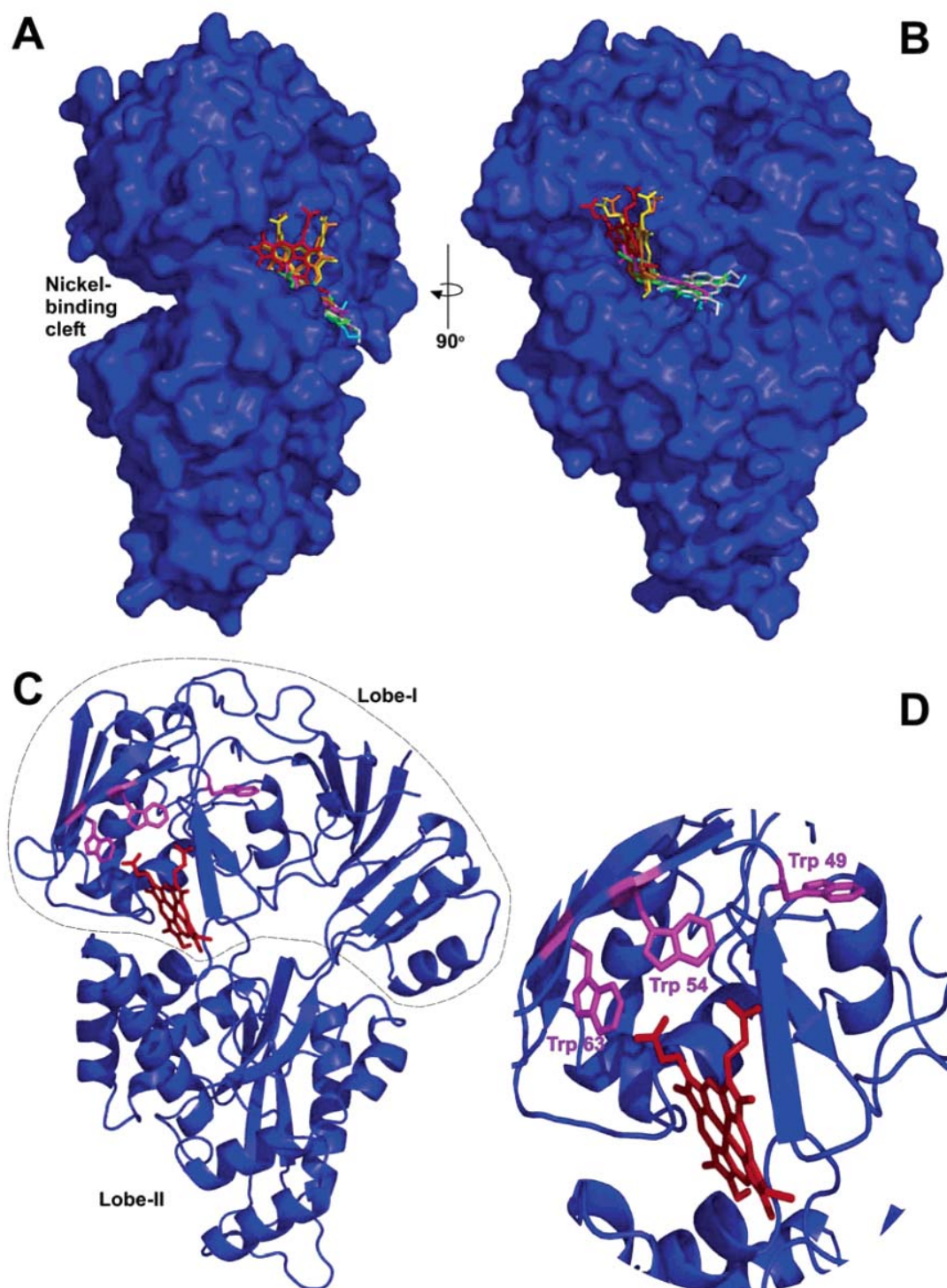


FIGURE 5: Models for a heme–NikA complex. Heme was docked onto the unliganded NikA structure (15) using ZDOCK (28). Half of the predicted complexes depicted heme docked in a cleft remote from the active site. The heme ligands are overlaid to demonstrate the clustering of these predicted complexes. Panels A and B depict the same complexes, except that panel B is rotated 90° in the vertical plane. (C) A cartoon depiction of one of the complexes in panel B, where the heme is adjacent to three tryptophan residues. (D) A magnified version of the complex in panel C.

and the P-574 signal may arise as a result of a reduced heme–NikA complex.

A recent crystal structure of *E. coli* NikA demonstrates the binding of $\text{FeEDTA}(\text{H}_2\text{O})^-$ (37) at the site previously shown to bind nickel (15), and the authors proposed that this chelated metal complex could be modeled into the original structure. Although EDTA cannot be the natural

chelator, they proposed that this structure could mimic a natural metallophore for nickel. This prompted a response from the Heddle group with a paper describing an additional structure and calorimetric data to reconcile this apparent conflict of results (38). That paper demonstrates that free nickel and chelated nickel ions bind to distinct sites on NikA, with K_d values of 11 and 30 μM , respectively. The

fluorescence quenching titrations in Figure 3 indicate that NikA may bind to heme and protoporphyrin in a manner independent of Ni^{2+} . Since 100 μM Ni^{2+} was used, these experiments were performed in the presence and absence of high concentrations of free nickel, even if a small concentration of EDTA was present from the purification. Hence, these data suggest that heme does not compete with free nickel when binding to NikA.

Periplasmic binding proteins (PBPs) in bacteria generally exhibit little sequence similarity, although sequence homology exists among NikA, *E. coli* DppA (dipeptide binding protein) (15), and *Haemophilus influenzae* HbpA (heme binding protein) (39). Heme has previously been docked into the substrate-binding cleft of a modeled structure of HbpA (based on the crystal structure of DppA) (40). Since *H. influenzae* imports heme, HbpA was tentatively assigned a role in heme transport, although it was later shown that HbpA had a role in heme utilization rather than heme acquisition (41). Also, it has recently been demonstrated that two NikA homologues, DppA and MppA (L-alanyl- γ -D-glutamyl-mesodiaminopimelate periplasmic binding protein), play similar roles in the uptake of heme in *E. coli* for use as an iron source (42). This study also reported that knocking out the *nikA* gene did not affect heme iron utilization, although other roles for a heme–NikA complex were not considered. The reported binding constants were approximately 10 and 50 μM for DppA and MppA, respectively. These values are greater than 10-fold higher than that of NikA, indicating weaker interactions with heme and probably reflecting a different role for heme binding of these PBPs to that of NikA.

The fluorescence quenching titrations in Figure 3 indicate that NikA may bind to heme and protoporphyrin in a manner independent of Ni^{2+} . This is consistent with the binding sites in Figure 5, which are remote from the nickel-binding cleft. Panel B shows seven of the predicted complexes. The hemes colored red, yellow, and orange are bound to lobe I of NikA, close to three tryptophan residues (panel D). This is consistent with the quenching of intrinsic tryptophan fluorescence upon heme binding. Furthermore, the more horizontal purple, cyan, white, and green hemes are bound at the interface of the two lobes, an area subject to large conformational changes during nickel binding (15). Since nickel does not appear to affect the binding affinity of heme or protoporphyrin (Figure 3), the red, yellow, and orange hemes in Figure 5 occupy a more likely binding site for a NikA–heme complex. However, future crystallization studies of the NikA–heme complex may elucidate the exact mode of binding.

At first inspection, the binding of heme and nickel by NikA appears to provide no common function. However, the assembly of the anaerobic hydrogenase isoenzymes may explain why NikA has evolved to bind both heme and nickel. The hydrogenase-1 and hydrogenase-2 isozymes of *E. coli* are encoded by the *hyaABCDE* (43) and *hyoOABCDEFG* (44, 45) operons, respectively. Both are involved in periplasmic hydrogen uptake. The hydrogenase-1 isozyme comprises both a Ni-containing catalytic subunit (HyaB) (46) and a putative membrane-bound cytochrome *b* γ subunit (HyaC) (47), although the exact function and composition of the latter protein remain unclear. The hydrogenase-2 isozyme resembles the hydrogen–quinone oxidoreductase system from sulfate-reducing bacteria (47), which utilizes a

16-heme cytochrome as a redox partner (48, 49), the reduction of which is mediated by cytochrome *c*₃. These observations suggest that hydrogenase activity in *E. coli* is dependent on both nickel- and heme-binding proteins. The *nik* operon is required for the delivery of nickel to the [NiFe] catalytic center of the hydrogenase enzyme (7–9). Our work may reflect a heme delivery role for NikA for the assembly of cytochromes associated with the hydrogenase isozymes of *E. coli*.

ACKNOWLEDGMENT

We are very grateful to Prof. Jeremy Tame (Yokohama City University, Yokohama, Japan) for supplying the pET28b-*nikA* construct used for the overexpression of NikA.

REFERENCES

1. Frausto da Silva, J. J. R., and Williams, R. J. P. (1991) *Biological Chemistry of the Elements: The Inorganic Chemistry of Life*, Oxford University Press, Oxford, U.K.
2. Panek, H., and O'Brian, M. R. (2002) A whole genome view of prokaryotic haem biosynthesis, *Microbiology* 148, 2273–2282.
3. Schulz, H., Hennecke, H., and Thony-Meyer, L. (1998) Prototype of a heme chaperone essential for cytochrome *c* maturation, *Science* 281, 1197–1200.
4. Stevens, J. M., Uchida, T., Daltrop, O., Kitagawa, T., and Ferguson, S. J. (2006) Dynamic ligation properties of the *Escherichia coli* heme chaperone CcmE to non-covalently bound heme, *J. Biol. Chem.* 281, 6144–6151.
5. Itagaki, E., and Hager, L. P. (1966) Studies on cytochrome *b*₅₆₂ of *Escherichia coli*. I. Purification and crystallization of cytochrome *b*₅₆₂, *J. Biol. Chem.* 241, 3687–3695.
6. Mathews, F. S., Bethge, P. H., and Czerwinski, E. W. (1979) Structure of cytochrome *b*₅₆₂ from *Escherichia coli* at 2.5 Å resolution, *J. Biol. Chem.* 254, 1699–1706.
7. Wu, L. F., and Mandrand-Berthelot, M. A. (1986) Genetic and physiological characterization of new *Escherichia coli* mutants impaired in hydrogenase activity, *Biochimie* 68, 167–179.
8. Wu, L. F., Mandrand-Berthelot, M. A., Waugh, R., Edmonds, C. J., Holt, S. E., and Boxer, D. H. (1989) Nickel deficiency gives rise to the defective hydrogenase phenotype of *hydC* and *fir* mutants in *Escherichia coli*, *Mol. Microbiol.* 3, 1709–1718.
9. Navarro, C., Wu, L. F., and Mandrand-Berthelot, M. A. (1993) The *nik* operon of *Escherichia coli* encodes a periplasmic binding-protein-dependent transport-system for nickel, *Mol. Microbiol.* 9, 1181–1191.
10. Wu, L. F., Navarro, C., and Mandrand-Berthelot, M. A. (1991) The *hydC* region contains a multi-cistronic operon (*Nik*) involved in nickel transport in *Escherichia coli*, *Gene* 107, 37–42.
11. De Pina, K., Desjardin, V., Mandrand-Berthelot, M. A., Giordano, G., and Wu, L. F. (1999) Isolation and characterization of the *nikR* gene encoding a nickel-responsive regulator in *Escherichia coli*, *J. Bacteriol.* 181, 670–674.
12. Stohs, S. J., and Bagchi, D. (1995) Oxidative mechanisms in the toxicity of metal ions, *Free Radical Biol. Med.* 18, 321–336.
13. De Pina, K., Navarro, C., McWalter, L., Boxer, D. H., Price, N. C., Kelly, S. M., Mandrand-Berthelot, M. A., and Wu, L. F. (1995) Purification and characterization of the periplasmic nickel-binding protein NikA of *Escherichia coli* K12, *Eur. J. Biochem.* 227, 857–865.
14. Salins, L. L. E., Goldsmith, E. S., Ensor, C. M., and Daunert, S. (2002) A fluorescence-based sensing system for the environmental monitoring of nickel using the nickel binding protein from *Escherichia coli*, *Anal. Bioanal. Chem.* 372, 174–180.
15. Heddle, J., Scott, D. J., Unzai, S., Park, S. Y., and Tame, J. R. H. (2003) Crystal structures of the liganded and unliganded nickel-binding protein NikA from *Escherichia coli*, *J. Biol. Chem.* 278, 50322–50329.

16. Pittman, M. S., Corker, H., Wu, G. H., Binet, M. B., Moir, A. J. G., and Poole, R. K. (2002) Cysteine is exported from the *Escherichia coli* cytoplasm by CydDC, an ATP-binding cassette-type transporter required for cytochrome assembly, *J. Biol. Chem.* 277, 49841–49849.
17. Pittman, M. S., Robinson, H. C., and Poole, R. K. (2005) A Bacterial Glutathione Transporter (*Escherichia coli* CydDC) Exports Reductant to the Periplasm, *J. Biol. Chem.* 280, 32254–32261.
18. Poole, R. K., Hatch, L., Cleeter, M. W. J., Gibson, F., Cox, G. B., and Wu, G. H. (1993) Cytochrome *bd* biosynthesis in *Escherichia coli*: The sequences of the *cydC* and *cydD* genes suggest that they encode the components of an ABC membrane transporter, *Mol. Microbiol.* 10, 421–430.
19. Poole, R. K., Gibson, F., and Wu, G. H. (1994) The *cydD* gene-product, component of a heterodimeric ABC transporter, is required for assembly of periplasmic cytochrome *c* and of cytochrome *bd* in *Escherichia coli*, *FEMS Microbiol. Lett.* 117, 217–224.
20. Goldman, B. S., Gabbert, K. K., and Kranz, R. G. (1996) Use of heme reporters for studies of cytochrome biosynthesis and heme transport, *J. Bacteriol.* 178, 6338–6347.
21. Cook, G. M., Cruz-Ramos, H., Moir, A. J. G., and Poole, R. K. (2002) A novel haem compound accumulated in *Escherichia coli* overexpressing the *cydDC* operon, encoding an ABC-type transporter required for cytochrome assembly, *Arch. Microbiol.* 178, 358–369.
22. Falk, J. E. (1964) *Porphyrins and metalloporphyrins: Their general, physical and coordination chemistry, and laboratory methods*, Elsevier, Amsterdam.
23. Fuhrhop, J. H., and Smith, K. M. (1975) in *Porphyrins and Metalloporphyrins* (Smith, K. M., Ed.) pp 806, Elsevier, Amsterdam.
24. Gibson, F., Cox, G. B., Downie, J. A., and Radik, J. (1977) A mutation affecting a second component of the F_0 portion of the magnesium ion-stimulated adenosine-triphosphatase of *Escherichia coli* K12: The *uncC424* allele, *Biochem. J.* 164, 193–198.
25. Studier, F. W. (1991) Use of bacteriophage T7 lysozyme to improve an inducible T7 expression system, *J. Mol. Biol.* 219, 37–44.
26. Qi, S. Y., Moir, A. J. G., and O'Connor, D. (1996) Proteome of *Salmonella typhimurium* SL1344: Identification of novel abundant cell envelope proteins and assignment to a two-dimensional reference map, *J. Bacteriol.* 178, 5032–5038.
27. Zelent, B., Kusba, J., Gryczynski, I., Johnson, M. L., and Lakowicz, J. R. (1998) Time-resolved and steady-state fluorescence quenching of *N*-acetyl-L-tryptophanamide by acrylamide and iodide, *Biophys. Chem.* 73, 53–75.
28. Chen, R., and Weng, Z. (2002) Docking unbound proteins using shape complementarity, desolvation, and electrostatics, *Proteins* 47, 281–294.
29. Silhavy, T. J., Szmecman, S., Boos, W., and Schwartz, M. (1975) Significance of retention of ligand by protein, *Proc. Natl. Acad. Sci. U.S.A.* 72, 2120–2124.
30. Thony-Meyer, L. (2000) Haem-polypeptide interactions during cytochrome *c* maturation, *Biochim. Biophys. Acta* 1459, 316–324.
31. Fabianek, R. A., Hennecke, H., and Thony-Meyer, L. (2000) Periplasmic protein thiol:disulfide oxidoreductases of *Escherichia coli*, *FEMS Microbiol. Rev.* 24, 303–316.
32. Kranz, R., Lill, R., Goldman, B., Bonnard, G., and Merchant, S. (1998) Molecular mechanisms of cytochrome *c* biogenesis: Three distinct systems, *Mol. Microbiol.* 29, 383–396.
33. Page, M. D., Sambongi, Y., and Ferguson, S. J. (1998) Contrasting routes of *c*-type cytochrome assembly in mitochondria, chloroplasts and bacteria, *Trends Biochem. Sci.* 23, 103–108.
34. Itagaki, E., Palmer, G., and Hager, L. P. (1967) Studies on cytochrome *b₅₆₂* of *Escherichia coli*. 2. Reconstitution of cytochrome *b₅₆₂* from apoprotein and hemin, *J. Biol. Chem.* 242, 2272–2277.
35. Low, D. W., Hill, M. G., Carrasco, M. R., Kent, S. B. H., and Botti, P. (2001) Total synthesis of cytochrome *b₅₆₂* by native chemical ligation using a removable auxiliary, *Proc. Natl. Acad. Sci. U.S.A.* 98, 6554–6559.
36. Deng, H. T. (2006) Characterization of the reaction products of cytochrome *c* with glutathione by mass spectrometry, *Biochem. Biophys. Res. Commun.* 342, 73–80.
37. Cherrier, M. V., Martin, L., Cavazza, C., Jacquamet, L., Lemaire, D., Gaillard, J., and Fontecilla-Camps, J. C. (2005) Crystallographic and spectroscopic evidence for high affinity binding of FeEDTA(H₂O)[−] to the periplasmic nickel transporter NikA, *J. Am. Chem. Soc.* 127, 10075–10082.
38. Addy, C., Ohara, M., Kawai, F., Kidera, A., Ikeguchi, M., Fuchigami, S., Osawa, M., Shimada, I., Park, S. Y., Tame, J. R. H., and Heddle, J. G. (2007) Nickel binding to NikA: An additional binding site reconciles spectroscopy, calorimetry and crystallography, *Acta Crystallogr. D* 63, 221–229.
39. Abouhamad, W. N., and Manson, M. D. (1994) The dipeptide permease of *Escherichia coli* closely resembles other bacterial transport-systems and shows growth-phase-dependent expression, *Mol. Microbiol.* 14, 1077–1092.
40. Duntun, P., and Mowbray, S. L. (1995) Modeling of the structure of the *Haemophilus influenzae* heme-binding protein suggests a mode of heme interaction, *Protein Sci.* 4, 2335–2340.
41. Morton, D. J., Madore, L. L., Smith, A., VanWagoner, T. M., Seale, T. W., Whitby, P. W., and Stull, T. L. (2005) The heme-binding lipoprotein (HbpA) of *Haemophilus influenzae*: Role in heme utilization, *FEMS Microbiol. Lett.* 253, 193–199.
42. Letoffe, S., Delepelaire, P., and Wandersman, C. (2006) The housekeeping dipeptide permease is the *Escherichia coli* heme transporter and functions with two optional peptide binding proteins, *Proc. Natl. Acad. Sci. U.S.A.* 103, 12891–12896.
43. Menon, N. K., Robbins, J., Peck, H. D., Chatelus, C. Y., Choi, E. S., and Przybyla, A. E. (1990) Cloning and sequencing of a putative *Escherichia coli* [NiFe] Hydrogenase-1 operon containing 6 open reading frames, *J. Bacteriol.* 172, 1969–1977.
44. Sargent, F., Ballantine, S. P., Rugman, P. A., Palmer, T., and Boxer, D. H. (1998) Reassignment of the gene encoding the *Escherichia coli* hydrogenase 2 small subunit: Identification of a soluble precursor of the small subunit in a *hypB* mutant, *Eur. J. Biochem.* 255, 746–754.
45. Menon, N. K., Chatelus, C. Y., Dervartanian, M., Wendt, J. C., Shanmugam, K. T., Peck, H. D., and Przybyla, A. E. (1994) Cloning, sequencing, and mutational analysis of the *hyb* operon encoding *Escherichia coli* hydrogenase-2, *J. Bacteriol.* 176, 4416–4423.
46. Sawers, R. G., and Boxer, D. H. (1986) Purification and properties of membrane-bound hydrogenase isoenzyme-1 from anaerobically grown *Escherichia coli*-K12, *Eur. J. Biochem.* 156, 265–275.
47. Dubini, A., Pye, R. L., Jack, R. L., Palmer, T., and Sargent, F. (2002) How bacteria get energy from hydrogen: A genetic analysis of periplasmic hydrogen oxidation in *Escherichia coli*, *Int. J. Hydrogen Energy* 27, 1413–1420.
48. Pereira, I. A. C., Romao, C. V., Xavier, A. V., LeGall, J., and Teixeira, M. (1998) Electron transfer between hydrogenases and mono- and multiheme cytochromes in *Desulfovibrio* spp., *J. Biol. Inorg. Chem.* 3, 494–498.
49. Dolla, A., Pohorelec, B. K. J., Voordouw, J. K., and Voordouw, G. (2000) Deletion of the *hmc* operon of *Desulfovibrio vulgaris* subsp. *vulgaris* Hildenborough hampers hydrogen metabolism and low-redox-potential niche establishment, *Arch. Microbiol.* 174, 143–151.
50. Poole, R. K., Williams, H. D., Downie, J. A., and Gibson, F. (1989) Mutations affecting the cytochrome-*d*-containing oxidase complex of *Escherichia coli* K12: Identification and mapping of a 4th locus, *cydD*, *J. Gen. Microbiol.* 135, 1865–1874.

BI700183U